Pure Appl. Geophys. 169 (2012), 1847–1858

DOI 10.1007/s00024-011-0449-1

Pure and Applied Geophysics

Analytical Solutions Involving Shock Waves for Testing Debris Avalanche Numerical Models

Sudi Mungkasi[1,2] and Stephen Gwyn Roberts[1]

Abstract—Analytical solutions to debris avalanche problems involving shock waves are derived. The debris avalanche problems are described in two different coordinate systems, namely, the standard Cartesian and topography-linked coordinate systems. The analytical solutions can then be used to test debris avalanche numerical models. In this article, finite volume methods are applied as the numerical models. We compare the performance of the finite volume method with reconstruction of the conserved quantities based on stage, height, and velocity to that of the conserved quantities based on stage, height, and momentum for solving the debris avalanche problems involving shock waves. The numerical solutions agree with the analytical solution. In addition, both reconstructions lead to similar numerical results. This article is an extension of the work of Mangeney et al. (Pure Appl Geophys 157(6–8):1081–1096, 2000).

Key words: Dam break, debris avalanche, method of characteristics, sloping topography, finite volume method, shock waves.

1. Introduction

Avalanche problems including rocks, snows, debris, lands (landslides), water, etc., have been studied using the Saint-Venant approach (shallow water wave equations) by a number of researchers (Mangeney *et al*. 2000; Mungkasi and G Roberts 2011c; Naaim *et al*. 1997; Stoker 1948, 1957) on a planar topography. Other than avalanche problems, the Saint-Venant model has a number of applications, such as for modelling in dam break, flood, tsunami, etc. The mathematical model of shallow water waves was originally derived by de Saint-Venant (1871). Readers interested in the derivation of shallow water models for arbitrary topography are referred to the work of Bouchut and Westdickenberg (2004). In addition, those interested in solving avalanche problems using a modified Saint-Venant model called the Savage–Hutter model are referred to the work of Tai *et al*. (2002).

Some research on dam break and debris avalanche problems using the Saint-Venant model is as follows. Ritter (1892) and Stoker (1948, 1957) solved the problems for the case with horizontal topography, particularly called the dam break problem. Mangeney *et al*. (2000) derived an analytical solution to the debris avalanche problem in a topography-linked coordinate system involving a dry area, where the wall separating quiescent wet and dry areas initially is not vertical, but orthogonal to the topography. Because a non-vertical dam is less similar to some real-world scenarios (Ancey *et al*. 2008), Mungkasi and Roberts (2011c) studied a modified problem having a vertical wall initially and developed its solution in the standard Cartesian coordinate system.

Mangeney *et al*. (2000) and Mungkasi and Roberts (2011c) derived solutions to debris avalanche problems only for cases involving wet and dry regions, that is, one region either on the left or right to the separating wall is dry. In their works, no discontinuous solution was involved. However, it is well known that because the model is hyperbolic, the Saint-Venant model admits a discontinuous solution called a bore or shock (shock wave) or hydraulic jump. This was also stated by Mangeney *et al*. (2000), which means that the study of debris avalanche problems using a Saint-Venant approach will be complete if a shock is included. Therefore, in this article, we consider problems on inclined slopes involving wet and wet regions, that is, both regions on the left and right of the initially separating wall are wet. With this setting, a shock will be formed as the

[1] Mathematical Sciences Institute, Australian National University, Canberra, Australia. E-mail: sudi.mungkasi@anu.edu.au; stephen.roberts@anu.edu.au

[2] Department of Mathematics, Sanata Dharma University, Yogyakarta, Indonesia.

time evolves (Stoker 1957). We apply the method of characteristics and a transformation technique to obtain the analytical solution to the debris avalanche problem involving a shock.

Two problems are considered. The first is the debris avalanche problem in the standard Cartesian coordinate system, as shown in Fig. 1, and the second is the debris avalanche problem in the topography-linked coordinate system, as shown in Fig. 2. We derive the analytical solutions to both problems having quiet state initially (zero initial velocity). Assuming that h_1 and h_0 are nonnegative representing the fluid heights on the left and right respectively of the separating wall given initially, we see that these two problems are the generalisations of those solved by Stoker (1948, 1957), Mangeney *et al.* (2000), and Mungkasi and Roberts (2011c). Note that for the case with a horizontal topography, these two problems coincide and Stoker (1948, 1957) has already solved it; for the case with an inclined topography and $h_1 = 0$ in the topography-linked coordinate system, Mangeney *et al.* (2000) have proposed a solution; the case with an inclined topography and $h_1 = 0$ in the standard Cartesian coordinate system has been recently solved by Mungkasi and Roberts (2011c).

The remainder of this article is organised as follows. Section 2 recalls the governing equations of debris flows in the standard Cartesian coordinate system, derives the analytical solution of the corresponding debris avalanche problem, and presents the properties of the analytical solution. Section 3 recalls the governing equations and develops the analytical solution of the debris avalanche problem in the topography-linked coordinate system. In Sect. 4, we use the analytical solution in the standard Cartesian coordinate system to test debris avalanche numerical models. Finally, some concluding remarks are provided in Sect. 5.

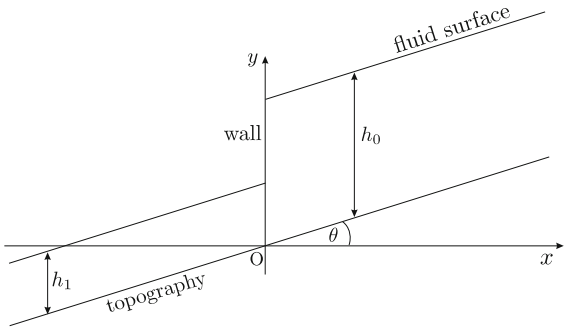

Figure 1
Initial profile of the debris avalanche problem in the standard Cartesian coordinate system

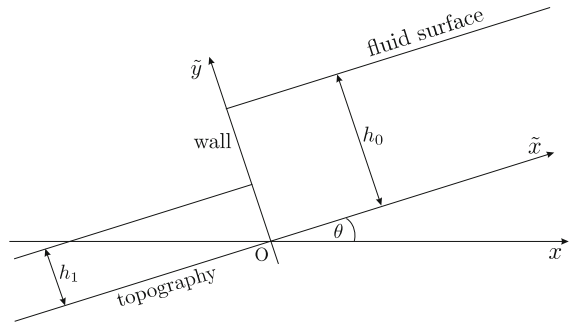

Figure 2
Initial profile of the debris avalanche problem in the topography-linked coordinate system

2. Debris Avalanche Problem in the Standard Cartesian Coordinate System

Consider the debris avalanche problem in the standard Cartesian coordinate system shown in Fig. 1. In this section, we recall the governing equations of fluid flows in the standard Cartesian coordinate system, derive the solution to the debris avalanche problem using characteristics and a transformation, and present the properties of the solution.

2.1. Governing Equations

In the standard Cartesian coordinate system, the mass and momentum equations governing the fluid motion are

$$\frac{\partial h}{\partial t} + \frac{\partial (hu)}{\partial x} = 0, \tag{1}$$

$$\frac{\partial (hu)}{\partial t} + \frac{\partial \left(hu^2 + \frac{1}{2}gh^2\right)}{\partial x} = -gh\frac{\mathrm{d}z}{\mathrm{d}x} + hF. \tag{2}$$

These two equations are called the Saint-Venant model or the shallow water equations. Here, x represents the coordinate in one-dimensional space, t represents the time variable, $u = u(x, t)$ denotes the fluid velocity, $h = h(x, t)$ denotes the fluid height,

$z = z(x)$ is the topography, and g is the acceleration due to gravity. In addition, F is a factor representing the Coulomb-type friction defined as

$$F = -g \cos^2\theta \tan\delta \operatorname{sgn} u \tag{3}$$

in the standard Cartesian coordinate system. This Coulomb-type friction is adapted from the one used by Mangeney *et al.* (2000). For further reference, we use the notations δ for representing the dynamic friction angle, θ for the angle between the topography (bed elevation) and the horizontal line, and w for the quantity $h + z$ called the stage. In this article, the values $\tan\delta$ and $\tan\theta$ are called the friction slope and bed slope respectively. Note that in the standard Cartesian coordinate system, we limit our discussion on the problems having bed topography $z(x)$ with property $\mathrm{d}z/\mathrm{d}x = \tan\theta$, where θ is constant.

Following Mangeney *et al.* (2000), we limit our discussion to the case when the friction slope is not larger than the bed slope, that is, $\tan\delta \leq \tan\theta$. With this limitation, after the separating wall is broken, the fluid motion never stops.Consequently, the Coulomb-type friction (3) can be simplified into

$$F = g \cos^2\theta \tan\delta \tag{4}$$

for the debris avalanche problem in the standard Cartesian coordinate system for time $t > 0$.

Taking Eq. 1 into account, we can rewrite Eq. 2 as

$$\frac{\partial u}{\partial t} + u\frac{\partial u}{\partial x} = -g\frac{\partial h}{\partial x} - g\tan\theta + F. \tag{5}$$

Introducing a "wave speed"[1] defined as

$$c = \sqrt{gh}, \tag{6}$$

and replacing h by c, we can rewrite Eqs. 1 and 5 to be

$$2\frac{\partial c}{\partial t} + 2u\frac{\partial c}{\partial x} + c\frac{\partial u}{\partial x} = 0, \tag{7}$$

$$\frac{\partial u}{\partial t} + u\frac{\partial u}{\partial x} + 2c\frac{\partial c}{\partial x} + g\tan\theta - F = 0. \tag{8}$$

An addition of Eqs. 7 to 8 and subtraction of Eqs. 7 from 8 result in

$$\left\{\frac{\partial}{\partial t} + (u + c)\frac{\partial}{\partial x}\right\} \cdot (u + 2c - mt) = 0, \tag{9}$$

$$\left\{\frac{\partial}{\partial t} + (u - c)\frac{\partial}{\partial x}\right\} \cdot (u - 2c - mt) = 0, \tag{10}$$

respectively, where

$$m = -g\tan\theta + F. \tag{11}$$

Note that this value of m is the horizontal acceleration of a particle sliding down an inclined topography (Dressler 1958; Mungkasi and Roberts 2011c).

In other words, Eqs. 1 and 2 are equivalent to characteristic relations

$$C_+ : \frac{\mathrm{d}x}{\mathrm{d}t} = u + c, \tag{12}$$

$$C_- : \frac{\mathrm{d}x}{\mathrm{d}t} = u - c, \tag{13}$$

in which

$$u + 2c - mt = k_+ = \text{constant along each curve } C_+, \tag{14}$$

$$u - 2c - mt = k_- = \text{constant along each curve } C_-, \tag{15}$$

where $m = -g\tan\theta + F$ and $c = \sqrt{gh}$. These $k_\pm$ are usually called the Riemann invariants.

2.2. Derivation of the Analytical Solution

Recall the debris avalanche problem shown in Fig. 1. In this subsection, we derive the analytical solution of this problem using characteristics. This method of characteristics for the Saint-Venant model is actually an adaptation of the method implemented by Courant and Friedrich (1948) in studying gas dynamics.

Figure 1 illustrates the fluid profile at time $t = 0$, while Fig. 3 shows the fluid motion and its characteristics at time $t > 0$. Note that Fig. 3 is a schematic illustration of the flow adapted from the work of Stoker (1957) and Mangeney *et al.* (2000), and is really the physics. At time $t = 0$, only two regions exist: Zone (1) has a linear surface with height h_1 on the left of the separating wall; and Zone (0) has a linear surface with height h_0 on the right. At time $t > 0$, four regions exist: Zone (1) is the linear surface

[1] Following Stoker (1957), we prefer to call c the wave speed (instead of the wave velocity), as it measures the propagation speed of the wave relative to the fluid velocity u. Moreover, the value of c is always nonnegative by definition, whereas the value of velocity could be negative or nonnegative.

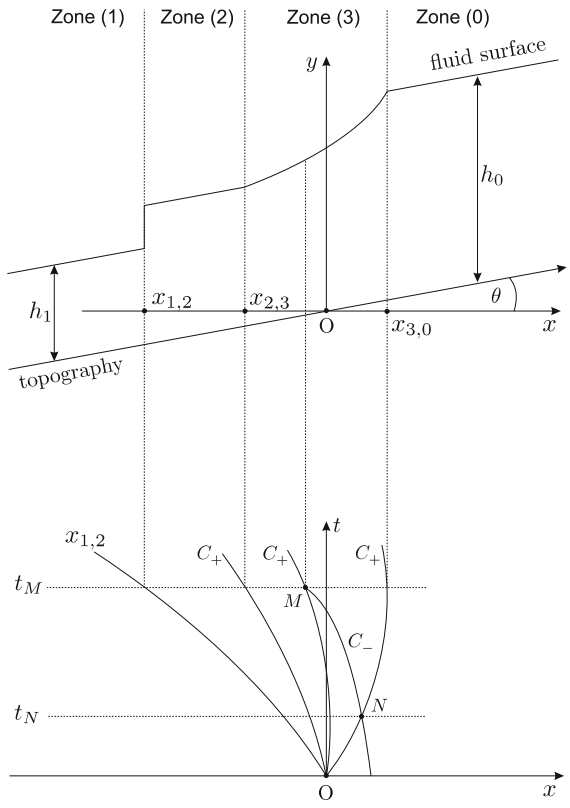

Figure 3
A schematic profile of the debris avalanche problem in the topography-linked coordinate system and their corresponding characteristic curves

with a constant height h_1; Zone (2) is another linear surface with constant height h_2; Zone (3) has a quadratic surface with height h_3; Zone (0) is the linear surface with height h_0. For time $t > 0$, we name $x_{1,2}$ as the point separating Zone (1) and Zone (2); $x_{2,3}$ as the point separating Zone (2) and Zone (3); and similarly $x_{3,0}$ separating Zone (3) and Zone (0). Zones (1) and (0) are the quiet regions, that is, the fluid is affected only by the acceleration due to gravity and remains unaffected by disturbance. Zones (2) and (3) are the disturbance regions, where the solutions in terms of height h and velocity u need to be found.

For further reference, we use the following conventions. For the arbitrary value of m, we use notations in Zones (1), (3), and (0) as follows: the velocity, height, and wave speed are denoted respectively by u_i, h_i, and c_i, where $i = 1, 3, 0$; the subscripts of the variables represent the name of the zone. For Zone (2), we denote the velocity, height, and wave speed by u_2, h_2, and c_2 only for the case when $m = 0$, and we state those quantities explicitly if we have $m \neq 0$. In addition, still in Zone (2), the shock velocity is denoted by σ only for the case when $m = 0$, and we also state it explicitly if the case is $m \neq 0$. Note that the shock position is exactly at the interface between Zones (1) and (2).

Recall that Zones (1) and (0) are the quiet regions, that is, the fluid is affected only by the acceleration due to gravity. Therefore, the heights at Zones (1) and (0) remain h_1 and h_0 respectively, and their corresponding velocities are the same value given by $u_1 = u_0 = mt$.

The solution at Zone (3) having a quadratic profile is derived in a similar way to our previous work (Mungkasi and Roberts 2011c) as follows. On the rightmost characteristic curve C_+ emanating from the origin, we have a velocity $u = at$ and relative wave speed $c_0 = \sqrt{gh_0}$. So, at arbitrary point N on that curve, we have a velocity $u = at_N$ and relative wave speed $c = c_0$ where t_N is the time associated with point N. Now, consider an arbitrary point M in zone II such that $t_M > t_N$, where t_M is the time associated with point M. Since k_- is constant along characteristic curve C_- passing through points M and N, and we have $a = m$, the velocity at point M is

$$u = 2c - 2c_0 + mt, \tag{16}$$

where t_M is rewritten as t for simplicity. The slope

$$\frac{\mathrm{d}x}{\mathrm{d}t} = u + c = 3c - 2c_0 + mt \tag{17}$$

is the slope of each characteristic curve C_+ in the rarefaction fan. Since k_+ is constant along each curve defined by $\mathrm{d}x/\mathrm{d}t = u + c$ and since the velocity u is given by (16), the relative wave speed c is constant along each curve in the rarefaction fan. As a result, Eq. 17 can be integrated to get

$$c = \frac{1}{3}\left(\frac{x}{t} + 2c_0 - \frac{1}{2}mt\right) \tag{18}$$

that is

$$h = \frac{1}{9g}\left(\frac{x}{t} + 2c_0 - \frac{1}{2}mt\right)^2. \tag{19}$$

Substituting (18) into (16), we obtain

$$u = \frac{2}{3}\left(\frac{x}{t} - c_0 + mt\right). \tag{20}$$

The position of $x_{3,0}$ is characterised by

$$\frac{\mathrm{d}x}{\mathrm{d}t} = u_0 + c_0 = mt + c_0. \tag{21}$$

Therefore, $x_{3,0} = c_0 t + \frac{1}{2}mt^2$.

Suppose that we have $m = 0$, so we have the classical dam break problem. The solution at Zone (2) is derived as follows. After the separating wall is removed ($t > 0$), a shock occurs. The shock position is at $x_{1,2}$, at the interface between Zone (1) and Zone (2). Let us denote the shock velocity as σ, which is a constant, so that the shock position is $x_{1,2} = \sigma\ t$ at time t. The shock conditions[2] are (Stoker 1957)

$$-\sigma(u_2 - \sigma) = \frac{1}{2}\left(c_1^2 + c_2^2\right), \tag{22}$$

$$c_2^2(u_2 - \sigma) = -c_1^2\sigma. \tag{23}$$

Using Eq. 23, we eliminate c_2^2 from Eq. 22 resulting in the quadratic equation

$$\sigma(u_2 - \sigma)^2 + \frac{1}{2}c_1^2(u_2 - \sigma) - \frac{1}{2}c_1^2\sigma = 0. \tag{24}$$

From this quadratic equation, we have

$$u_2 = \sigma - \frac{c_1^2}{4\sigma}\left(1 + \sqrt{1 + 8\left(\frac{\sigma}{c_1}\right)^2}\right), \tag{25}$$

in which the positive sign (instead of the negative) in front of the square root is chosen such that $u_2 - \sigma$ and $-\sigma$ have the same sign. This same sign guarantees that Zone (2) expands out, as the time t evolves. Using Eq. 22, we eliminate u_2 from Eq. 64, and so

$$c_2 = c_1\sqrt{\frac{1}{2}\left(\sqrt{1 + 8\left(\frac{\sigma}{c_1}\right)^2} - 1\right)}, \tag{26}$$

is obtained. The shock conditions (22) and (23) now become (25) and (26). We see that infinitely many solutions exist satisfying (25) and (26), as there are three unknowns, namely u_2, c_2, and σ, but only two equations are given. To get a unique set of solutions, we need one more equation. The other equation is found by observing the characteristic curve passed by $x_{2,3}$. Recall that k_- is constant along each characteristic curve C_-. Therefore,

$$u - 2c - mt = -2c_0 \tag{27}$$

over the whole Zone (3), and

$$u - 2c - mt = u_2 - 2c_2 \tag{28}$$

at point $x_{2,3}$. As a result, we have

$$-2c_0 = u_2 - 2c_2 \tag{29}$$

at point $x_{2,3}$. Therefore, u_2, c_2, and σ are found by solving the three simultaneous Eqs. 25, 26, and 29.

If $m \neq 0$, at Zone (2), the quantities u_2 and σ defined for $m = 0$ described above must be corrected for the fluid velocity and shock velocity. Recall that the constant m is the horizontal acceleration of a particle sliding down an inclined topography. This implies that the fluid velocity and shock velocity at Zone (2) are $u_2 + mt$ and $\sigma + mt$ respectively. The position of $x_{2,3}$ is then characterised by

$$\frac{\mathrm{d}x}{\mathrm{d}t} = (u_2 + mt) + c_2, \tag{30}$$

which implies that $x_{2,3} = (u_2 + c_2)t + \frac{1}{2}mt^2$. In addition, the shock position is $x_{1,2} = \sigma t + \frac{1}{2}mt^2$.

Therefore, the solution to the debris avalanche problem in the standard Cartesian coordinate system is

$$h(x,t) = \begin{cases} h_1 & \text{if } x < \sigma t + \frac{1}{2}mt^2 \\ h_2 & \text{if } \sigma t + \frac{1}{2}mt^2 \le x < (u_2 + c_2)t + \frac{1}{2}mt^2 \\ \frac{1}{9g}\left(\frac{x}{t} + 2c_0 - \frac{1}{2}mt\right)^2 & \text{if } (u_2 + c_2)t + \frac{1}{2}mt^2 \le x < c_0 t + \frac{1}{2}mt^2 \\ h_0 & \text{if } x \ge c_0 t + \frac{1}{2}mt^2 \end{cases} \tag{31}$$

and

$$u(x,t) = \begin{cases} mt & \text{if } x < \sigma t + \frac{1}{2}mt^2 \\ u_2 + mt & \text{if } \sigma t + \frac{1}{2}mt^2 \le x < (u_2 + c_2)t + \frac{1}{2}mt^2 \\ \frac{2}{3}\left(\frac{x}{t} - c_0 + mt\right) & \text{if } (u_2 + c_2)t + \frac{1}{2}mt^2 \le x < c_0 t + \frac{1}{2}mt^2 \\ mt & \text{if } x \ge c_0 t + \frac{1}{2}mt^2 \end{cases} \tag{32}$$

for time $t > 0$. Here u_2, c_2, and σ are the solutions of the three simultaneous Eqs. 25, 26, and 29. The value of h_2 is calculated using relation $c_2 = \sqrt{gh_2}$.

[2] These shock conditions were derived by Stoker (1957) for the case when the topography is horizontal. In fact, the shock conditions for arbitrary shape of topography are still the same as long as the topography is continuous, as proved by Dressler (1949).

Alternatively, we can implement a transformation technique to get the solution to the debris avalanche problem by recalling the solution to the classical dam break problem. The solution, where $m = 0$ and $h_0 > h_1$, is (Stoker 1957)

$$h(x,t) = \begin{cases} h_1 & \text{if } x < \sigma t \\ h_2 & \text{if } \sigma t \le x < (u_2 + c_2)t \\ \frac{1}{9g}\left(\frac{x}{t} + 2c_0\right)^2 & \text{if } (u_2 + c_2)t \le x < c_0 t \\ h_0 & \text{if } x \ge c_0 t \end{cases} \tag{33}$$

and

$$u(x,t) = \begin{cases} 0 & \text{if } x < \sigma t \\ u_2 & \text{if } \sigma t \le x < (u_2 + c_2)t \\ \frac{2}{3}\left(\frac{x}{t} - c_0\right) & \text{if } (u_2 + c_2)t \le x < c_0 t \\ 0 & \text{if } x \ge c_0 t \end{cases} \tag{34}$$

for time $t > 0$. Here u_2, c_2, and σ are the solutions of the three simultaneous Eqs. 25, 26, and 29. The value of h_2 is calculated using relation $c_2 = \sqrt{gh_2}$. Let us now review a transformation technique as follows. We consider the Saint-Venant model in the standard Cartesian coordinate system, (1) and (2), and denote that $m = -g\tan\theta + F$ and $c = \sqrt{gh}$. Introducing new variables (Mangeney *et al.* 2000; Mungkasi and Roberts 2011c; Watson *et al.* 1992)

$$\xi = x - \frac{1}{2}mt^2, \quad \tau = t, \quad \upsilon = u - mt, \quad H = h \tag{35}$$

into (1) and (2), we obtain

$$H_\tau + (\upsilon H)_\xi = 0, \tag{36}$$

$$(H\upsilon)_\tau + \left(H\upsilon^2 + \frac{1}{2}gH^2\right)_\xi = 0. \tag{37}$$

Therefore for a given initial condition, if the solution to (36) and (37) is

$$\upsilon = \upsilon(\xi,\tau), \quad \text{and} \quad H = H(\xi,\tau) \tag{38}$$

then the solution to (1) and (2) is

$$u(x,t) = \upsilon(\xi,t) + mt, \quad \text{and} \quad h(x,t) = H(\xi,t). \tag{39}$$

Consequently, the solution to the debris avalanche problem shown in Fig. 1, where $h_0 > h_1$, is (31) and (32) for time $t > 0$.

2.3. Properties of the Analytical Solution

In this subsection, we provide three properties of the analytical solution (31) and (32) we have derived to the debris avalanche problem following the properties of the solution to the dam break problem presented by Stoker (1957).

The first is the property of the solution at point $x = \frac{1}{2}mt^2$. If

$$u_2 + c_2 + mt \le 0, \tag{40}$$

this point $x = \frac{1}{2}mt^2$ belongs to Zone (3), and we have that at this point the fluid height, velocity, and momentum are

$$h = \frac{4}{9}h_0, \quad u = -\frac{2}{3}c_0, \quad p = -\frac{8}{27}h_0c_0, \tag{41}$$

respectively. If

$$u_2 + c_2 + mt > 0, \tag{42}$$

the point $x = \frac{1}{2}mt^2$ belong to Zone (2), and we see that the fluid height, velocity, and momentum at this point are

$$h = h_2, \quad u = u_2 + mt, \quad p = h_2(u_2 + mt), \tag{43}$$

respectively.

The second is the height of the shock, measured by $h_2 - h_1$. The height of the shock is zero when $h_1 = 0$ or $h_1 = h_0$, and it attains its maximum $h_2 - h_1 = 0.32\,h_0$ when $h_1/h_0 = 0.176$, as described by Stoker (1957).

The third is the behaviour of the solution when $h_1 = h_0$ or $h_1 = 0$. Recalling the solution given by (31) and (32), and its illustration in Fig. 3, we describe the behaviour as follows. When $h_1 = h_0$, the height of the shock is zero, which corresponds to the fact that the shock speed σ equals the value of the fluid velocity upstream u_0. At the same time, Zone (3) disappears, as the width of Zone (3) is zero. We note that when $h_1 = h_0$, what happens is just a block of fluid sliding downstream with a constant height h_0 and velocity $u = mt$. For the other case, when $h_1 = 0$, the analytical solution (31) and (32) becomes:

$$h(x,t) = \begin{cases} 0 & \text{if } x < -2c_0t + \frac{1}{2}mt^2 \\ \frac{1}{9g}\left(\frac{x}{t} + 2c_0 - \frac{1}{2}mt\right)^2 & \text{if } -2c_0t + \frac{1}{2}mt^2 \le x < c_0t + \frac{1}{2}mt^2 \\ h_0 & \text{if } x \ge c_0t + \frac{1}{2}mt^2 \end{cases} \tag{44}$$

and

$$u(x,t) = \begin{cases} 0 & \text{if } x < -2c_0t + \frac{1}{2}mt^2 \\ \frac{2}{3}\left(\frac{x}{t} - c_0 + mt\right) & \text{if } -2c_0t + \frac{1}{2}mt^2 \le x < c_0t + \frac{1}{2}mt^2 \\ mt & \text{if } x \ge c_0t + \frac{1}{2}mt^2 \end{cases} \tag{45}$$

that is, the analytical solution derived by MUNGKASI and ROBERTS (2011c) to the debris avalanche problem involving a dry bed in the standard Cartesian coordinate system. When $h_1 = 0$, we say that there is not a shock in the solution. This is because when $h_1 = 0$, Zone (2) is squeezed out into one point, which is the interface between wet and dry areas, and the dry area is always reached by the rarefaction wave.

3. Debris Avalanche Problem in the Topography-Linked Coordinate System

Consider the debris avalanche problem in the topography-linked coordinate system shown in Fig. 2. In this section, we recall the governing equations and briefly derive the analytical solution to the problem.

3.1. Governing Equations

In the topography-linked coordinate system, the Saint-Venant model written in the conservative form with a flat topography is

$$\frac{\partial \tilde{h}}{\partial t} + \frac{\partial(\tilde{h}\tilde{u})}{\partial \tilde{x}} = 0, \tag{46}$$

$$\frac{\partial(\tilde{h}\tilde{u})}{\partial t} + \frac{\partial\left(\tilde{h}\tilde{u}^2 + \frac{1}{2}g\tilde{h}^2\cos\theta\right)}{\partial \tilde{x}} = -\tilde{h}\left(g\sin\theta - \tilde{F}\right). \tag{47}$$

Equations 46 and 47 are the equation of mass and that of momentum respectively. Here, $\tilde{x}$ represents the coordinate in one-dimensional space, t represents the time variable, $\tilde{u} = \tilde{u}(\tilde{x}, t)$ denotes the fluid velocity, $\tilde{h} = \tilde{h}(\tilde{x}, t)$ denotes the fluid height, θ is the angle between the topography (bed elevation) and the horizontal line, and g is the acceleration due to gravity. In addition, $\tilde{F}$ is a factor representing the Coulomb-type friction, given by

$$\tilde{F} = -g\cos\theta\tan\delta\,\mathrm{sgn}\tilde{u} \tag{48}$$

in this topography-linked coordinate system. Recall that we use the notation δ for representing the dynamic friction angle, and the values $\tan\delta$ and $\tan\theta$ are the friction slope and bed slope respectively.

Again, following MANGENEY *et al.* (2000), we limit our discussion to the case when $\tan\delta \le \tan\theta$, so the Coulomb-type friction is defined by

$$\tilde{F} = g\cos\theta\tan\delta, \tag{49}$$

for the debris avalanche problem in the topography-linked coordinate system for time $t > 0$. We use tilde ˜notation attached in the quantity variables for those variables corresponding to the problem in the topography-linked coordinate system, and the standard quantity variables (without tilde ˜ notation) are used for variables corresponding to the problem in the standard Cartesian coordinate system.

Taking Eq. 46 into account, we can rewrite Eq. 47 as[3]

$$\frac{\partial \tilde{u}}{\partial t} + \tilde{u}\frac{\partial \tilde{u}}{\partial \tilde{x}} = -g\cos\theta\frac{\partial \tilde{h}}{\partial \tilde{x}} - g\sin\theta + \tilde{F}. \tag{50}$$

Introducing a "wave speed" defined as

$$\tilde{c} = \sqrt{g\tilde{h}\cos\theta}, \tag{51}$$

MANGENEY *et al.* (2000) showed that Eqs. 46 and 50 can be rewritten as

$$2\frac{\partial \tilde{c}}{\partial t} + 2\tilde{u}\frac{\partial \tilde{c}}{\partial \tilde{x}} + \tilde{c}\frac{\partial \tilde{u}}{\partial \tilde{x}} = 0, \tag{52}$$

$$\frac{\partial \tilde{u}}{\partial t} + \tilde{u}\frac{\partial \tilde{u}}{\partial \tilde{x}} + 2\tilde{c}\frac{\partial \tilde{c}}{\partial \tilde{x}} + g\sin\theta - \tilde{F} = 0. \tag{53}$$

The value of $\tilde{c}$ is the wave speed relative to the fluid velocity $\tilde{u}$. An addition of (52) to (53) and subtraction of (52) from (53) result in

$$\left\{\frac{\partial}{\partial t} + (\tilde{u} + \tilde{c})\frac{\partial}{\partial \tilde{x}}\right\} \cdot (\tilde{u} + 2\tilde{c} - \tilde{m}t) = 0, \tag{54}$$

$$\left\{\frac{\partial}{\partial t} + (\tilde{u} - \tilde{c})\frac{\partial}{\partial \tilde{x}}\right\} \cdot (\tilde{u} - 2\tilde{c} - \tilde{m}t) = 0, \tag{55}$$

[3] Equations (1) and (2) in the paper of MANGENEY *et al.* (2000) were called "mass and momentum equations". We believe that it was a typographical error (misprint), as in their context, it should be written as "momentum and mass equations".

respectively, where

$$\tilde{m} = -g \sin\theta + \tilde{F}. \tag{56}$$

In other words, Eqs. 46 and 47 are equivalent to characteristic relations

$$\tilde{C}_+ : \frac{\mathrm{d}\tilde{x}}{\mathrm{d}t} = \tilde{u} + \tilde{c}, \tag{57}$$

$$\tilde{C}_- : \frac{\mathrm{d}\tilde{x}}{\mathrm{d}t} = \tilde{u} - \tilde{c}, \tag{58}$$

in which

$$\tilde{u} + 2\tilde{c} - \tilde{m}t = \tilde{k}_+ = \text{constant along each curve } \tilde{C}_+, \tag{59}$$

$$\tilde{u} - 2\tilde{c} - \tilde{m}t = \tilde{k}_- = \text{constant along each curve } \tilde{C}_-, \tag{60}$$

where $\tilde{m} = -g \sin\theta + \tilde{F}$, and $\tilde{c} = \sqrt{g\tilde{h}\cos\theta}$. These $\tilde{k}_\pm$ are the Riemann invariants.

From Eqs. 12–15 and 57–60, we see that the problems in the topography-linked coordinate system are analogous to those in the standard Cartesian coordinate system.

3.2. *Derivation and Properties of the Analytical Solution*

Because the debris avalanche problem in the topography-linked coordinate system is analogous to that in the standard Cartesian coordinate system, methods applicable in the standard Cartesian coordinate system are also applicable in the topography-linked coordinate system. Therefore, we can use either characteristics or a transformation technique to solve the debris avalanche problem in the topography-linked coordinate system. For brevity, we solve the problem using a transformation.

Recall the solution (33) and (34) to the classical dam break problem. Introducing new variables

$$\tilde{\xi} = \tilde{x} - \frac{1}{2}\tilde{m}t^2, \quad \tau = t, \quad \tilde{\upsilon} = \tilde{u} - \tilde{m}t, \quad \tilde{H} = \tilde{h} \tag{61}$$

into (46) and (47), we can solve the problem in the transformed coordinate. The solution in the transformed coordinate is then transformed back to the original topography-linked coordinate so that the solution to the debris avalanche problem shown in Fig. 2, where $\tilde{h}_0 > \tilde{h}_1$, is

$$\tilde{h}(\tilde{x},t) = \begin{cases} \tilde{h}_1 & \text{if } \tilde{x} < \tilde{\sigma}t + \frac{1}{2}\tilde{m}t^2 \\ \tilde{h}_2 & \text{if } \tilde{\sigma}t + \frac{1}{2}\tilde{m}t^2 \le \tilde{x} < (\tilde{u}_2 + \tilde{c}_2)t + \frac{1}{2}\tilde{m}t^2 \\ \frac{1}{9g\cos\theta}\left(\frac{\tilde{x}}{t} + 2\tilde{c}_0 - \frac{1}{2}\tilde{m}t\right)^2 & \text{if } (\tilde{u}_2 + \tilde{c}_2)t + \frac{1}{2}\tilde{m}t^2 \le \tilde{x} < \tilde{c}_0 t + \frac{1}{2}\tilde{m}t^2 \\ \tilde{h}_0 & \text{if } \tilde{x} \ge \tilde{c}_0 t + \frac{1}{2}\tilde{m}t^2 \end{cases} \tag{62}$$

and

$$\tilde{u}(\tilde{x},t) = \begin{cases} \tilde{m}t & \text{if } \tilde{x} < \tilde{\sigma}t + \frac{1}{2}\tilde{m}t^2 \\ \tilde{u}_2 + \tilde{m}t & \text{if } \tilde{\sigma}t + \frac{1}{2}\tilde{m}t^2 \le \tilde{x} < (\tilde{u}_2 + \tilde{c}_2)t + \frac{1}{2}\tilde{m}t^2 \\ \frac{2}{3}\left(\frac{\tilde{x}}{t} - \tilde{c}_0 + \tilde{m}t\right) & \text{if } (\tilde{u}_2 + \tilde{c}_2)t + \frac{1}{2}\tilde{m}t^2 \le \tilde{x} < \tilde{c}_0 t + \frac{1}{2}\tilde{m}t^2 \\ \tilde{m}t & \text{if } \tilde{x} \ge \tilde{c}_0 t + \frac{1}{2}\tilde{m}t^2 \end{cases} \tag{63}$$

for time $t > 0$. Here $\tilde{u}_2, \tilde{c}_2$, and $\tilde{\sigma}$ are the solutions of three simultaneous equations

$$\tilde{u}_2 = \tilde{\sigma} - \frac{\tilde{c}_1^2}{4\tilde{\sigma}}\left(1 + \sqrt{1 + 8\left(\frac{\tilde{\sigma}}{\tilde{c}_1}\right)^2}\right), \tag{64}$$

$$\tilde{c}_2 = \tilde{c}_1\sqrt{\frac{1}{2}\left(\sqrt{1 + 8\left(\frac{\tilde{\sigma}}{\tilde{c}_1}\right)^2} - 1\right)}, \tag{65}$$

$$-2\tilde{c}_0 = \tilde{u}_2 - 2\tilde{c}_2 \tag{66}$$

where $\tilde{m} = -g \sin\theta + \tilde{F}$. Note that $\tilde{c}_i = \sqrt{g\tilde{h}_i \cos\theta}$, $i = 1, 2, 3, 0$. The value of $\tilde{h}_2$ is calculated using relation $\tilde{c}_2 = \sqrt{g\tilde{h}_2 \cos\theta}$.

The properties of this solution are similar to those of the solution to the debris avalanche problem in the standard Cartesian coordinate system. In particular, if $\tilde{h}_1 = 0$, the analytical solution (62) and (63) becomes:

$$\tilde{h}(\tilde{x},t) = \begin{cases} \tilde{h}_1 & \text{if } \tilde{x} < -2\tilde{c}_0 t + \frac{1}{2}\tilde{m}t^2 \\ \frac{1}{9g\cos\theta}\left(\frac{\tilde{x}}{t} + 2\tilde{c}_0 - \frac{1}{2}\tilde{m}t\right)^2 & \text{if } -2\tilde{c}_0 t + \frac{1}{2}\tilde{m}t^2 \le \tilde{x} < \tilde{c}_0 t + \frac{1}{2}\tilde{m}t^2 \\ \tilde{h}_0 & \text{if } \tilde{x} \ge \tilde{c}_0 t + \frac{1}{2}\tilde{m}t^2 \end{cases} \tag{67}$$

and

$$\tilde{u}(\tilde{x},t) = \begin{cases} \tilde{m}t & \text{if } \tilde{x} < -2\tilde{c}_0 t + \frac{1}{2}\tilde{m}t^2 \\ \frac{2}{3}\left(\frac{\tilde{x}}{t} - \tilde{c}_0 + \tilde{m}t\right) & \text{if } -2\tilde{c}_0 t + \frac{1}{2}\tilde{m}t^2 \le \tilde{x} < \tilde{c}_0 t + \frac{1}{2}\tilde{m}t^2 \\ \tilde{m}t & \text{if } \tilde{x} \ge \tilde{c}_0 t + \frac{1}{2}\tilde{m}t^2 \end{cases} \tag{68}$$

that is, the analytical solution derived by MANGENEY *et al.* (2000) to the debris avalanche problem involving a dry bed in the topography-linked coordinate system. However, we argue that the analytical solution (62) and (63) and that of MANGENEY *et al.* (2000) are not valid physically. This is because for cases with steep bed slopes, some material at the top around the wall given in Fig. 2 would fall down and collapse with some material from around point O moving to the left soon after the wall is removed (MUNGKASI and ROBERTS 2011c). This collapse should have a defect in the solution. For this reason, it is better for us to use the solution to the debris avalanche problem in the standard Cartesian coordinate system to test debris avalanche numerical models.

4. Numerical Models

In this section, we test finite volume numerical models (finite volume methods) used to solve the debris avalanche problem. We compare the performance of Method A (the finite volume method with reconstruction based on stage $w := h + z$, height h, and velocity u) to that of Method B (the finite volume method with reconstruction based on stage w, height h, and momentum $p := hu$) in solving the debris avalanche problem involving a shock.

The numerical scheme is described as follows. The Saint-Venant model (1) and (2) can be written in a vector form

$$\mathbf{q}_t + \mathbf{f}(\mathbf{q})_x = \mathbf{s} \tag{69}$$

where the vectors of quantity $\mathbf{q}$, flux function $\mathbf{f}$, and source term $\mathbf{s}$ are

$$\mathbf{q} = \begin{bmatrix} h \\ hu \end{bmatrix}, \quad \mathbf{f} = \begin{bmatrix} hu \\ hu^2 + \frac{1}{2}gh^2 \end{bmatrix}, \quad \text{and} \quad \mathbf{s} = \begin{bmatrix} 0 \\ -ghz_x + hF \end{bmatrix}. \tag{70}$$

Taking the hydrostatic reconstruction (AUDUSSE *et al.* 2004; NOELLE *et al.* 2006)

$$z^*_{i+\frac{1}{2}} := \max\{z_{i,r}, z_{i+1,l}\}, \tag{71}$$

$$h^*_{i,r} := \max\{0, h_{i,r} + z_{i,r} - z^*_{i+\frac{1}{2}}\}, \tag{72}$$

$$h^*_{i+1,l} := \max\{0, h_{i+1,l} + z_{i+1,l} - z^*_{i+\frac{1}{2}}\} \tag{73}$$

we have that the values for h^* lead to auxiliary values for the conserved quantities, $\mathbf{Q}^* = (h^*, h^*u)^T$. Then, a semi-discrete well-balanced finite volume scheme for the Saint-Venant model in the standard Cartesian coordinate system is

$$\begin{aligned} \Delta x_i \frac{\mathrm{d}}{\mathrm{d}t}\mathbf{Q}_i &+ \mathcal{F}^r(\mathbf{Q}_i, \mathbf{Q}_{i+1}, z_{i,r}, z_{i+1,l}) \\ &- \mathcal{F}^l(\mathbf{Q}_{i-1}, \mathbf{Q}_i, z_{i-1,r}, z_{i,l}) \\ &= \mathbf{S}_i^{(j)} \end{aligned} \tag{74}$$

where the right and left numerical fluxes of the ith cell are respectively calculated at $x_{i+1/2}$ and $x_{i\text{-}1/2}$, and

$$\mathcal{F}^r(\mathbf{Q}_i, \mathbf{Q}_{i+1}, z_{i,r}, z_{i+1,l}) := \mathbf{F}(\mathbf{Q}^*_{i,r}, \mathbf{Q}^*_{i+1,l}) + \mathbf{S}_{i,r}, \tag{75}$$

and

$$\mathcal{F}^l(\mathbf{Q}_{i-1}, \mathbf{Q}_i, z_{i-1,l}, z_{i,r}) := \mathbf{F}(\mathbf{Q}^*_{i-1,r}, \mathbf{Q}^*_{i,l}) + \mathbf{S}_{i,l}. \tag{76}$$

Here, $\mathbf{Q}$ is the approximation of the vector $\mathbf{q}$, and $\mathbf{F}$ is a conservative numerical flux consistent with the homogeneous shallow water wave equations computed in such a way that the method is stable. In addition,

$$\mathbf{S}_{i,r} := \begin{bmatrix} 0 \\ \frac{g}{2}h^2_{i,r} - \frac{g}{2}(h^*_{i,r})^2 \end{bmatrix}, \quad \mathbf{S}_{i,l} := \begin{bmatrix} 0 \\ \frac{g}{2}h^2_{i,l} - \frac{g}{2}(h^*_{i,l})^2 \end{bmatrix} \tag{77}$$

are the corrections due to the water height modification in the hydrostatic reconstruction. Furthermore, the index j of $\mathbf{S}_i^{(j)}$ in Eq. 74 denotes the order of the numerical source term. The first and second order numerical source terms are

$$\begin{aligned} \mathbf{S}_i^{(1)} &:= \begin{bmatrix} 0 \\ h_i F \end{bmatrix} \quad \text{and} \\ \mathbf{S}_i^{(2)} &:= \begin{bmatrix} 0 \\ -g\frac{h_{i,r}+h_{i,l}}{2}(z_{i,r} - z_{i,l}) + h_i F \end{bmatrix}, \end{aligned} \tag{78}$$

where F is defined by (3). This scheme is based on the well-balanced finite volume scheme proposed by AUDUSSE *et al.* (2004) and extended to higher orders of accuracy by NOELLE *et al.* (2006).

In all simulations, the numerical settings are as follows. We use the second-order source, second-order spatial, and second-order temporal discretizations. The central upwind flux formulation proposed by KURGANOV *et al.* (2001) is used to compute the

numerical fluxes. Quantities are measured in SI units. The acceleration due to gravity is taken as $g = 9.81$. The minmod limiter is applied in the quantity reconstruction, and we note that this limiter leads the numerical method to a total variation diminishing (TVD) method (LeVeque 2002). The Courant-Friedrichs-Lewy number used in the simulations is 1.0. The spatial domain is $[-100, 100]$. The initial fluid heights are $h_1 = 5$ on the left and $h_0 = 10$ on the right of the wall. The discrete L^1 absolute error (Mungkasi and Roberts 2010, 2011a, c)

$$E = \frac{1}{N}\sum_{i=1}^{N}|q(x_i) - Q_i| \tag{79}$$

is used to quantify numerical error, where N is the number of cells, q is the exact quantity function, x_i is the centroid of the ith cell, and Q_i is the average value of quantity of the ith cell produced by the numerical method.

The simulations are done in Python 2.4. In order that our solvers can be reached and used by the community, we have uploaded the codes of our analytical and numerical solvers on http://sites.google.com/a/dosen.usd.ac.id/sudi_mungkasi/research/codes/Avalanche.rar. Similar numerical solvers have also been tested for solving the Saint-Venant model in our previous work (Mungkasi and Roberts 2010, 2011a, b for the case without friction and Mungkasi and Roberts 2011c for the case with friction).

Three test cases are considered. First, we test the numerical methods for a problem with friction slope $\tan\delta = 0$ and bed slope $\tan\theta = 0$. Table 1 shows errors for stage w, momentum p and velocity u with various number of cells for this first case. Second, we consider a problem with friction slope $\tan\delta = 0$ and bed slope $\tan\theta = 0.1$. Table 2 presents errors for stage w, momentum p, and velocity u with various number of cells for this second case. Finally, for the third case we consider a problem with friction slope $\tan\delta = 0.05$ and bed slope $\tan\theta = 0.1$. The errors for stage w, momentum p, and velocity u with various numbers of cells are presented in Table 3. For this third case, Fig. 4 shows the debris avalanche consisting of stage w, momentum p, and velocity u at time $t = 5$ using Method B with 400 cells. Method A results in a similar figure.

Table 1

Errors for $\tan\delta = 0$ *and* $\tan\theta = 0$ *at* $t = 5$

Number of cells	w error		p error		u error	
	A	B	A	B	A	B
100	0.0525	0.0522	0.4592	0.4566	0.0602	0.0599
200	0.0280	0.0280	0.2531	0.2530	0.0318	0.0318
400	0.0146	0.0147	0.1337	0.1343	0.0167	0.0168
800	0.0067	0.0067	0.0599	0.0600	0.0077	0.0077
1,600	0.0033	0.0033	0.0296	0.0297	0.0038	0.0038

Table 2

Errors for $\tan\delta = 0$ *and* $\tan\theta = 0.1$ *at* $t = 5$

Number of cells	w error		p error		u error	
	A	B	A	B	A	B
100	0.0662	0.0659	0.6348	0.6280	0.0732	0.0725
200	0.0324	0.0322	0.2987	0.2944	0.0364	0.0360
400	0.0165	0.0164	0.1518	0.1504	0.0186	0.0185
800	0.0083	0.0083	0.0764	0.0756	0.0094	0.0094
1,600	0.0041	0.0041	0.0382	0.0378	0.0047	0.0047

Table 3

Errors for $\tan\delta = 0.05$ *and* $\tan\theta = 0.1$ *at* $t = 5$

Number of cells	w error		p error		u error	
	A	B	A	B	A	B
100	0.0582	0.0576	0.4983	0.4921	0.0658	0.0651
200	0.0301	0.0300	0.2664	0.2642	0.0339	0.0337
400	0.0152	0.0152	0.1360	0.1353	0.0172	0.0172
800	0.0077	0.0077	0.0693	0.0692	0.0087	0.0087
1,600	0.0039	0.0039	0.0358	0.0359	0.0045	0.0045

Several remarks can be drawn from the numerical results. From the error comparison shown in Tables 1, 2, and 3, we see that Methods A and B perform[4] similarly. To be specific we could say that Method B results in slightly smaller error, but the difference between the results of Methods A and B is indeed insignificant. In addition, according to Tables 1, 2, and 3, as the cell length is halved, the errors produced by the numerical methods are halved. This means that we have only a first order of convergence, even though we have used second-order methods. This is

[4] In the simulations for the debris avalanche problem involving a dry area (Mungkasi and Roberts 2011c), Method B resulted in a slightly smaller error.

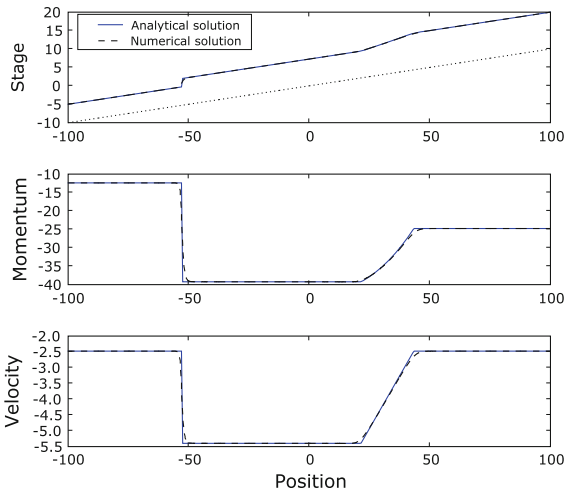

Figure 4
Stage, momentum, and velocity for avalanche with $\tan\delta = 0.05$, $\tan\theta = 0.1$, at $t = 5$, using Method B where the spatial domain is descretized into 400 cells. The *dotted line* in the *first subfigure* represents the bed topography

due to diffusions around the shock and the corners in the numerical solution, as shown in Fig. 4. It is well known in the numerical analysis of conservation laws that in the presence of a shock or discontinuity, finite volume methods (second-order TVD methods in our case here) converge at most with first-order accuracy (Leon *et al*. 2007; LeVeque 1992).

5. Conclusions

We have used the shallow water approach to solve the debris avalanche problems. The analytical solution to the problems in the standard Cartesian coordinate system has been used for testing the performance of two finite volume numerical models having different ways of reconstructing the conserved quantities. Numerical results show that both reconstructions lead to the same accuracy when the numerical models are used to solve the one-dimensional debris avalanche problem involving a shock for the parameter settings considered.

Acknowledgments

The work of Sudi Mungkasi was supported by ANU PhD and ANU Tuition Scholarships.

References

C. Ancey, R. M. Iverson, M. Rentschler, R. P. Denlinger, 2008. *An exact solution for ideal dam-break floods on steep slopes*, Water Resources Research, *44*(W01430): 1–10.

E. Audusse, F. Bouchut, M. O. Bristeau, R. Klein, B. Perthame, 2004. *A fast and stable well-balanced scheme with hydrostatic reconstruction for shallow water flows*, SIAM Journal on Scientific Computing, *25*(6): 2050–2065.

F. Bouchut, M. Westdickenberg, 2004. *Gravity driven shallow water models for arbitrary topography*, Communications in Mathematical Sciences, *2*(3): 359–389.

R. Courant, K. O. Friedrichs, *Supersonic Flow and Shock Waves*, Interscience Publishers, New York, 1948.

A. J. C. de Saint-Venant, 1871. *Theorie du mouvement non-permanent des eaux, avec application aux crues des rivieres et a l'introduction des marees dans leur lits*, C. R. Acad. Sc. Paris, *73*: 147–154.

R. F. Dressler, 1949. *Mathematical solution of the problem of roll-waves in inclined open channels*, Communications on Pure and Applied Mathematics, *2*(2–3): 149–194.

R. F. Dressler, 1958. *Unsteady non-linear waves in sloping channels*, Proc. Royal Soc. London, Ser. A, *247*(1249): 186–198.

A. Kurganov, S. Noelle, G. Petrova, 2001. *Semidiscrete central-upwind schemes for hyperbolic conservation laws and Hamilton-Jacobi equations*, SIAM Journal on Scientific Computing, *23*(3): 707–740.

A. S. Leon, M. S. Ghidaoui, A. R. Schmidt, M. H. Garcia, An efficient finite-volume scheme for modeling water hammer flows, in W. James (Ed.) *Stormwater and urban water systems modeling conference, Toronto, 2006: Contemporary modeling of urban water systems, Monograph 15*, pp. 411–430, CHI, Guelph, 2007.

R. J. LeVeque, *Numerical methods for conservation laws*, Birkhauser, Basel, 1992.

R. J. LeVeque, *Finite volume methods for hyperbolic problems*, Cambridge University Press, Cambridge, 2002.

A. Mangeney, P. Heinrich, R. Roche, 2000. *Analytical solution for testing debris avalanche numerical models*, Pure and Applied Geophysics, *157*(6–8): 1081–1096.

S. Mungkasi, S. G. Roberts, 2010. *On the best quantity reconstructions for a well balanced finite volume method used to solve the shallow water wave equations with a wet/dry interface*, ANZIAM Journal, *51*(EMAC2009): C48–C65.

S. Mungkasi, S. G. Roberts, 2011a. *Approximations of the Carrier-Greenspan periodic solution to the shallow water wave equations for flows on a sloping beach*, International Journal for Numerical Methods in Fluids, in press http://dx.doi.org/10.1002/fld.2607, 18 pages.

S. Mungkasi, S. G. Roberts, 2011b. *Numerical entropy production for shallow water flows*, ANZIAM Journal, *52*(CTAC2010): C1–C17.

S. Mungkasi, S. G. Roberts, 2011c. *A new analytical solution for testing debris avalanche numerical models*, ANZIAM Journal, *52*(CTAC2010): C349–C363.

M. Naaim, S. Vial, R. Couture, *Saint Venant approach for rock avalanches modelling*, in Proceedings of Saint Venant Symposium: Multiple scale analyses and coupled physical systems, pp. 61–69, Presse Ecole Natl. Ponts Chaussees, Paris, 1997.

S. Noelle, N. Pankratz, G. Puppo, J. R. Natvig, 2006. *Well-balanced finite volume schemes of arbitrary order of accuracy for*

shallow water flows, Journal of Computational Physics, *213*(2): 474–499.

A. Ritter, 1892. *Die fortpflanzung der wasserwellen*, Zeitschrift des Vereines Deutscher Ingenieure, *36*(33): 947–954.

J. J. Stoker, 1948. *The formation of breakers and bores*, Communications on Pure and Applied Mathematics, *1*(1): 1–87.

J. J. Stoker, *Water Waves: The Mathematical Theory with Application*, Interscience Publishers, New York, 1957.

Y. C. Tai, S. Noelle, J. M. N. T. Gray, K. Hutter, 2002. *Shock-capturing and front-tracking methods for granular avalanches*, Journal of Computational Physics, *175*(1): 269–301.

G. Watson, D. H. Peregrine, E. F. Toro, *Numerical solution of the shallow-water equations on a beach using the weighted average flux method*, Proceedings of First European Computational Fluid Dynamics Conference, Brussels, 7–11 September 1992: Computational Fluid Dynamics '92 Vol.1, pp. 495–502, Elsevier, Amsterdam, 1992.

(Received July 12, 2011, revised October 7, 2011, accepted November 16, 2011, Published online January 11, 2012)